Turkish Journal of Biology

Volume 39 | Number 4 Article 7

1-1-2015

Optimization of multiplex RT-PCR for M1, M23, and M23X splice variants of AQP4 and ß-actin transcripts in Dalton?s lymphoma mouse tissues

RAJANEESH KUMAR GUPTA

SUKALA PRASAD

TÜBİTAK

Turkish Journal of Biology

http://journals.tubitak.gov.tr/biology/

Research Article

Turk J Biol
(2015) 39: 567-574
© TÜBİTAK
doi:10.3906/biy-1410-57

Optimization of multiplex RT-PCR for M1, M23, and M23X splice variants of AQP4 and β-actin transcripts in Dalton's lymphoma mouse tissues

Rajaneesh Kumar GUPTA, Sukala PRASAD*
Molecular Biology and Biochemistry Lab, Centre of Advanced Study in Zoology, Banaras Hindu University, Varanasi, Uttar Pradesh, India

Received: 29.10.2014 • **Accepted/Published Online:** 16.03.2015 • **Printed:** 30.07.2015

Abstract: Multiplex reverse transcriptase–polymerase chain reaction (MRT-PCR) is a method of choice for efficient and simultaneous analysis of gene expression at the transcript level with limited amounts of tissues; however, it is less common than other methods due to certain limitations. Here, we describe the protocol for MRT-PCR–based semiquantitative analysis of all AQP4 transcripts simultaneously in Dalton's lymphoma (DL) using transcript-specific primers and outline the critical parameters. Aquaporin-4 (AQP4) water channels are associated with edema of tissues due to various diseases. The AQP4 transcript possesses alternative transcription initiation sites and produces three isoforms, AQP4.M1, AQP4.M23, and AQP4.M23X, which constitute heterotetrameric orthogonal arrays of particles (OAPs) in the plasma membrane. In order to validate the MRT-PCR technique, the AQP4 transcripts were also analyzed in various tissues of mice with DL. β-Actin transcript was simultaneously amplified as a reference to monitor the possible intra- and interassay variations during MRT-PCR reactions and for relative quantification of target mRNAs. Our data suggest that the MRT-PCR technique is suitable for simultaneous detection and semiquantitative analysis of AQP4 transcripts, and can also be used as a routine tool for simultaneous analysis of multiple transcripts in other tissues.

Key words: MRT-PCR, AQP4, Dalton's lymphoma, gene expression, primer designing

1. Introduction

Altering expression of a gene is important for elucidating its function (Kurnaz, 2005). Polymerase chain reaction (PCR) is one of the cutting edge techniques that provide molecular biology research with a sensitive and rapid analysis of gene expression in tissues under various experimental or physiological conditions and requires a limited amount of tissue and time. The first description of PCR that was used for analysis of expression of a particular gene in a single reaction was reported by Kleppe et al. (1971). A second hedonistic innovation was provided by Mullis (1990). In the following years, its several variants have been used for molecular characterization of genes and diagnosing diseases (Bonab et al., 2012; Porob et al., 2013) and genetic diversity (Surgun et al., 2012). Multiplex RT-PCR (MRT-PCR) is the combination of the conversion of an mRNA into its cDNA (reverse transcription) and PCR. It encompasses analysis of multiple transcripts and tissue-specific gene expression in a single experiment (Crisan, 1994; Li et al., 2013; Tuo et al., 2014). The current manuscript focuses on the development of a step-by-step working protocol for MRT-PCR for quantification of alternative splice variants of AQP4 transcripts, and it has been tested in different nonlymphatic tissues of Dalton's lymphoma (DL)-bearing mice. DL is a transplantable T-cell lymphoma, a type of non-Hodgkin's lymphoma that begins in the lymphatic system, can be induced through ascites in rodents, and may influence nonlymphatic organs (Maurya and Vinayak, 2015). Detection of altered AQP4 mRNA levels in DL mice, which leads to dysregulation of water and ion homeostasis in various body organs, may be one of the events that make organs/cells edematous. Tissue hydration during cancer development is a process that might involve altered AQP4 expression (Papadoulos and Saadoun, 2014). According to Ma et al. (1996) three transcripts, AQP4.M1, AQP4.M23, and AQP4.M23X, are found in various mice tissues due to alternative splicing of AQP4 mRNA. Therefore, it could be interesting to observe the effects of lymphoma on differential expression of AQP4 transcripts in nonlymphatic tissues (brain, lung, and kidney) that abundantly express AQP4. In order to study the expression of AQP4 transcripts in mice altered by DL it may be helpful to understand mechanisms of the swelling of nonlymphatic tissues/cells during lymphoma.

* Correspondence: s.sprasadbhu@gmail.com

MRT-PCR is an important tool that saves time, and biological samples are used to check the expression profile of a battery of genes. However, it is difficult to standardize the whole technique; therefore, it requires optimizations at each step of MRT-PCR. Designing primers for MRT-PCR is a critical task that requires not only specificity but primer–primer compatibility, which is achieved only when each member of the primer pair anneals in a stable fashion to its target sequence in the template DNA without interfering with other primers and amplified products. Here, we report an optimized protocol to co-detect all AQP4 transcript variants by RT-PCR with the internal control β-actin in the same reaction system. This assay may help analyze AQP4 transcripts or others in pathological or experimentally treated samples, which could save time and may be cost effective.

2. Materials and methods

2.1. Maintenance of animals and sample collection

Adult male albino mice (20 weeks) of AKR strain (*Mus musculus*) were used for the experiments. They were fed with standard mouse feed, given drinking water ad libitum, and maintained at 25 ± 2 °C with a 12 h light/dark schedule in an isolated animal house. For animal maintenance, guidelines of the Committee for the Purpose of Control and Supervision on Experiments on Animals (CPCSEA), India (Gupta and Kanungo, 2013; Verma et al., 2013) were followed. Mice of the same age were used for inducing DL by transplantation of live lymphoma ascites. For induction of lymphoma, each mouse received ~5 × 10^6 cells/mL in normal saline through intraperitoneal injection. Control mice received only an equal volume of normal saline. After 15 days, control and DL-bearing mice were sacrificed. Then brain, lung, and kidney were dissected out and snap frozen in liquid nitrogen and stored at –80 °C.

2.2. Special equipment

- Thermal cycler (MJ mini, Bio-Rad, Hercules, CA, USA)
- Cooling centrifuge (Heraeus, Hanau, Germany)
- UV-Vis spectrophotometer (Jasco, Easton, MD, USA)
- UV transilluminator (Fotodyne, Hartland, WI, USA)
- Potter–Elvehjam type homogenizer (Remi Motors, Mumbai, India)
- UV light camera (Nikon, Tokyo, Japan)
- Gel casting apparatus and electrophoretic tank (Genie, Redmond, WA, USA)

2.3. Chemicals/reagents

- Agarose powder, diethylpyrocarbonate (DEPC), ethidium bromide, 3-(N-morpholino) propanesulfonic acid (MOPS), TRI reagent (Sigma, St Louis, MO, USA)
- Chloroform, ethanol, formaldehyde (Merck KGaA, Darmstadt, Germany)
- DNase-I (DNA free, Ambion, Austin, TX, USA)
- dNTP, random hexamer, RiboLock RNase inhibitor, RevertAid H minus M-MuLv reverse transcriptase, 2X RNA loading dye (MBI Fermentas, Burlington, ON, Canada)
- Mineral oil, Taq DNA polymerase (Genie, Redmond, WA, USA)
- DNA size markers (range: 100–1200 base pairs) (NEB, Beverly, MA, USA)

2.4. Experimental design

2.4.1. RNA extraction

Total RNA is recommended for RT-PCR when the sample is limited to minimize the differences in recovery and achieve a good quality template. RNA extraction from normal and DL mouse brain, lung, and kidney tissues was performed separately using the TRI reagent according to manufacturer's protocol. Total RNA was dissolved in DEPC-treated water and stored at –80 °C until use.

2.4.2. DNase-I digestion and RNA quantification

Total RNA was treated with DNase-I (DNA-free, Ambion), according to the manufacturer's guidelines, to remove any DNA contamination. RNA concentration was calculated by spectrophotometric measurement of absorbance at 260 nm after appropriate dilutions. The integrity of the RNA samples was verified by 1% formaldehyde agarose gel electrophoresis containing 20 mM MOPS, 8 mM Na-acetate, 1 mM EDTA, and 2.2 M formaldehyde (Gupta and Prasad, 2013; Gupta and Prasad, 2014).

2.4.3. Reverse transcription

Master Mix with appropriate reagents was preferred for reproducibility of cDNA synthesis. To synthesize the first strand of cDNA, 2 µg of total RNA and 200 ng of random hexamer primers were mixed, and reaction volume was made up to 11 µL. It was incubated at 70 °C for 5 min and chilled on ice. Thereafter, 2 µL of 5X reaction buffer, 2 µL of 10 mM dNTP mix, and 20 U of RNase inhibitor were added, and volume was made up to 19 µL. The tube was incubated for 5 min at 25 °C, and 200 U of MMuLV reverse transcriptase was added. The tube was incubated for 10 min at 25 °C and at 42 °C for 1 h in a thermal cycler. The reaction was terminated by heating at 70 °C for 10 min and chilling on ice, and the tube was stored at –70 °C or used directly for PCR reaction.

2.4.4. Primer designing

Primer3 (frodo.wi.mit.edu/primer3) was used to design gene-specific primers. Three sequence-specific forward primers and a common reverse primer were designed to amplify AQP4.M1, AQP4.M23, and AQP4.M23X amplicons (Figure 1). A separate pair of specific primers was designed to amplify the β-actin amplicon. The primer sequences were identified as transcript-specific using the basic local alignment search tool (BLAST; www.ncbi.nlm.nih.gov/BLAST) against gene bank databases. Primer

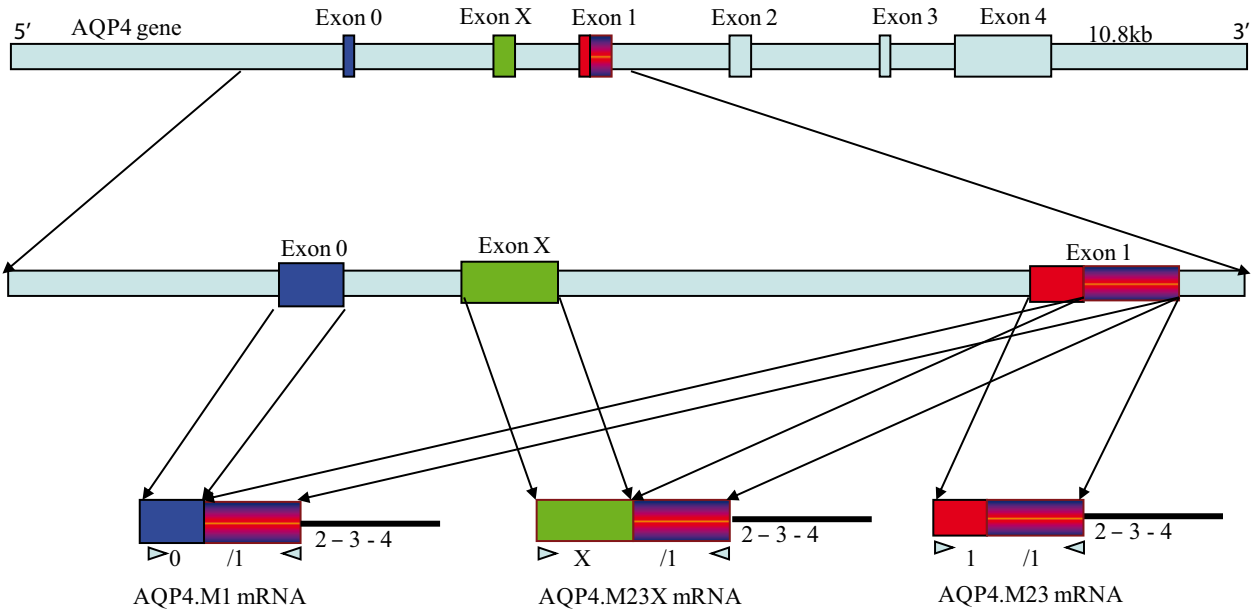

Figure 1. Schematic diagram illustrating primer positions to the AQP4 cDNA template to amplify AQP4.M1, AQP4.M23, and AQP4.M23X transcripts.

sequences were tested for possible interactions by using MultiPLX 2.0 (bioinfo.ebc.ee/multiPLX), as described on the web page.

2.4.5. Polymerase chain reaction (PCR)

Specific primers for PCR amplification were custom synthesized by Metabion International AG, Germany. The sequences, orientations, locations, and gene accession numbers of these primer sequences are outlined in the Table. The annealing temperatures and primer amounts were validated for proper amplification of each amplicon. The coamplification was carried out in a 50 µL reaction mixture containing 3 µL of cDNA, 5 µL of 10X Taq DNA polymerase buffer with 15 mM $MgCl_2$, 0.6 mM of each dNTP, 3 U of Taq DNA polymerase, and 10 pmol of AQP4 and β-actin forward and reverse primers. The samples were denatured at 94 °C for 5 min and amplified using the following amplification parameters: denaturation at 94 °C for 1 min, primer annealing at 60 °C for 1 min, and elongation at 72 °C for 1 min; the number of cycles was 29. The number of cycles used for coamplification was within the exponential phases of coamplification of all amplicons.

2.4.6 Analysis and quantification of coamplified products

The coamplified products were loaded on a 6% polyacrylamide (acrylamide:bisacrylamide, 29.3:0.7) gel and stained with DNA-intercalating ethidium bromide dye followed by destaining in dH_2O. The resulting gel bands were visualized in a UV-transilluminator and photographed by Nikon digital camera. Band intensity was analyzed by computer-assisted densitometry by Alpha Ease FC software version 3.1.2 (Alpha Innotech, CA, USA).

Table. Details of primer sequences used in the MSQ RT-PCR experiments to amplify AQP4.M1, AQP4M23, AQP4.M23X, and β-actin.

Transcripts	Primer sequences (5′→ 3′)	Genbank entry number	Location of primers cDNA sequence		Amplicon size (bp)
			Exons	Nucleotides	
AQP4.M1	Sense: AGTGCCCGTAATCTGACTCCCA	AF219992	Exon 0	54–75	519
AQP4.M23	Sense: GGAAGGCTAGGTTGGTGACTTC		Exon 1	122–143	460
AQP4.M23X	Sense: TTATGGTTCACGGGTTTGGATG		Exon X	6–27	749
	Antisense: TGGTGACTCCCAATCCTCCAAC		Exon 1	316– 338	
β-Actin	Sense: ATCGTGGGCCGCTCTAGGCACC	NM_007393	Exon 2	33–54	543
	Antisense: CTCTTTGATGTCACGCACGATTTC		Exon 4	416–431	

The relative expression level was measured by dividing the integrated density value (IDV) of target transcript bands by the IDV of β-actin bands, and the data were expressed as relative density values (RDVs). All experiments were repeated three times (n = 9). The IDV/RDV of bands on the gel represents the mean ± SEM of three data for each group.

2.4.7. Controls

The following were controls with all multiplex, semiquantitative RT-PCR experiments: (a) mock sample control with water in place of cDNA; (b) reverse transcriptase control, 2 µg of RNA in place of cDNA.

3. Results

3.1. Optimization of number of cycles for PCR coamplification

PCR coamplification was performed for 24–34 cycles for M1, M23, and M23X splice variants of AQP4 and β-actin transcripts, respectively. To achieve the overlapping exponential phase for all target amplicons, β-actin primers were added after ten cycles of M1, M23, and M23X amplification. The linear exponential phase was achieved for all target amplicons between 24 and 34 cycles (Figure 2).

3.2. Analysis of primer-primer compatibility

We performed di-, tri-, and tetraplexing PCR with the following combinations of primers: AQP4.M1 + β-actin, AQP4.M23 + β-actin, AQP4.M23X + β-actin, AQP4.M1 + AQP4.M23 + β-actin, AQP4.M1 + AQP4.M23X + β-actin, AQP4.M23 + AQP4.M23X + β-actin, and AQP4.M1 + AQP4.M23 + AQP4.M23X + β-actin. The normalized integrated density values were obtained and compared for every PCR reaction. We found that the ratios were not affected by other primers or amplified products (Figure 3).

3.3. Coamplification of AQP4 transcripts in non-lymphatic organs of DL mice

We found that in brain, lung, and kidney all mRNA levels were comparable at an adult age. As seen in Figures 4A and 4B, AQP4.M23X transcript is expressed at higher levels in the brain than in the kidney or lung. AQP4.M1 and AQP4.M23 transcripts were expressed at relatively high levels in the kidney and low levels in the lung and brain. This approach was also used to examine the effect of DL on the expression of AQP4 transcripts in brain, lung, and kidney. Compared with expression in normal brain, lung, and kidney tissues, the expression of AQP4.M23X transcript increased in lymphoma-affected brain. The expression of AQP4.M23 transcript increased in lymphoma-affected kidney and brain, whereas the expression of AQP4.M1 transcript increased in lymphoma-affected kidney and lung (Figures 4A and 4B).

4. Discussion

Gene expression studies have significantly enhanced our knowledge regarding regulation of gene expression and gene function in all areas of basic and applied life sciences. This is the first report on validation of coamplification

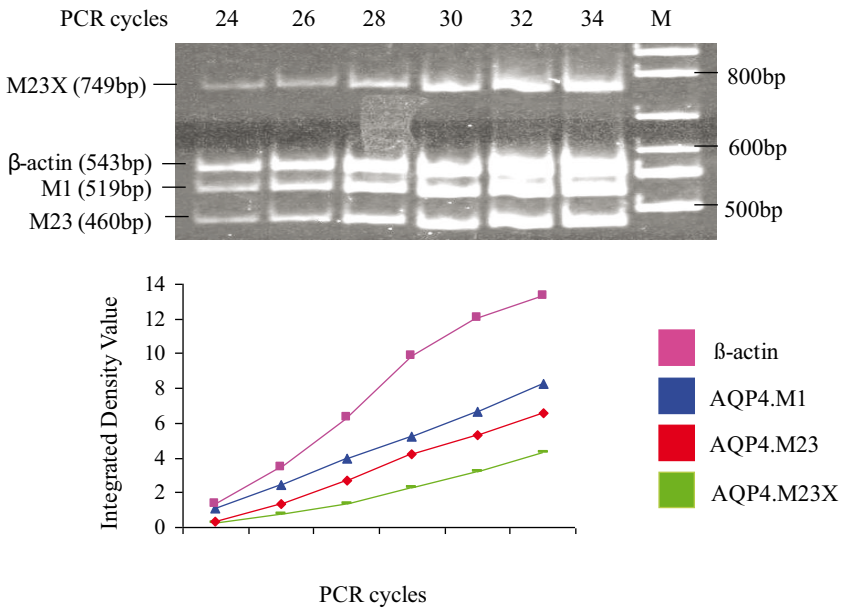

Figure 2. Optimization of PCR cycle number to determine the exponential phase of amplification reaction for AQP4.M1, AQP4.M23, AQP4.M23X, and β-actin amplicons. Integrated density values of the amplicons were obtained from different numbers of cycles. M denotes marker 100-bp DNA ladder.

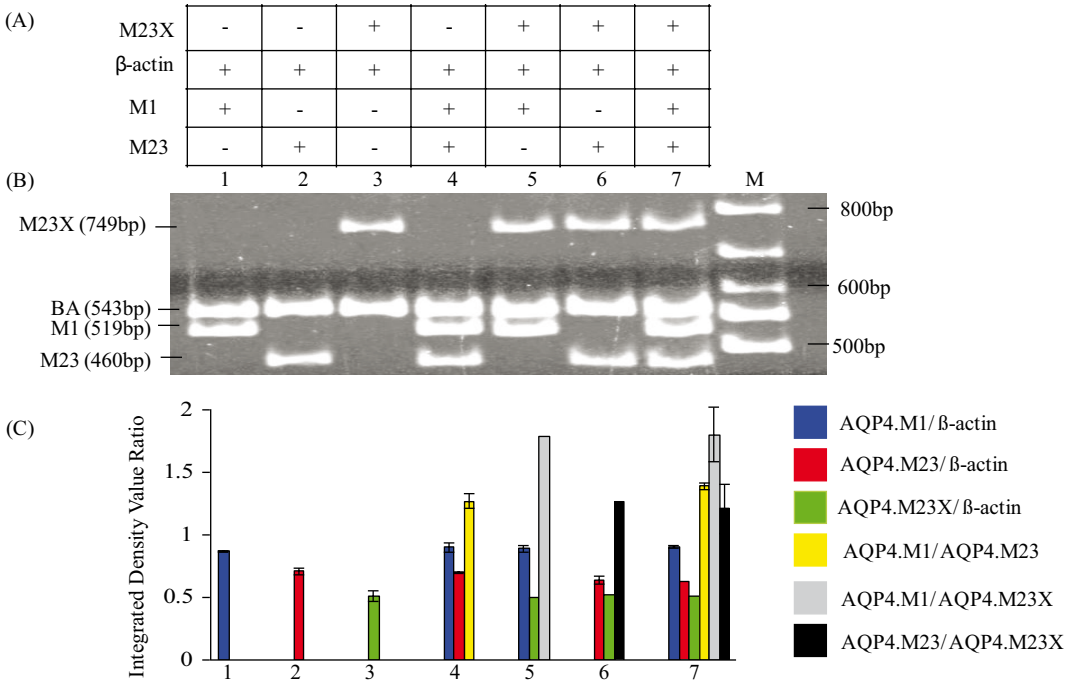

Figure 3. Primer-primer compatibility test. (A) Table showing the combinations of primer pairs: 1, AQP4.M1 + β-actin; 2, AQP4.M23 + β-actin; 3, AQP4.M23X + β-actin; 4, AQP4.M1 + AQP4.M23 + β-actin; 5, AQP4.M1 + AQP4.M23X + β-actin; 6, AQP4.M23 + AQP4.M23X + β-actin; and 7, AQP4.M1 + AQP4.M23 + AQP4.M23X + β-actin. (B) Gel showing the products of the primer combinations mentioned in A. The ratio between normalized integrated density values was obtained for every PCR reaction. The ratio was not affected by other primers or amplified products. (C) Bar diagram represents the ratio of normalized integrated density value for various combinations of primer pairs from three independent experiments ± SEM. M denotes marker 100-bp DNA ladder.

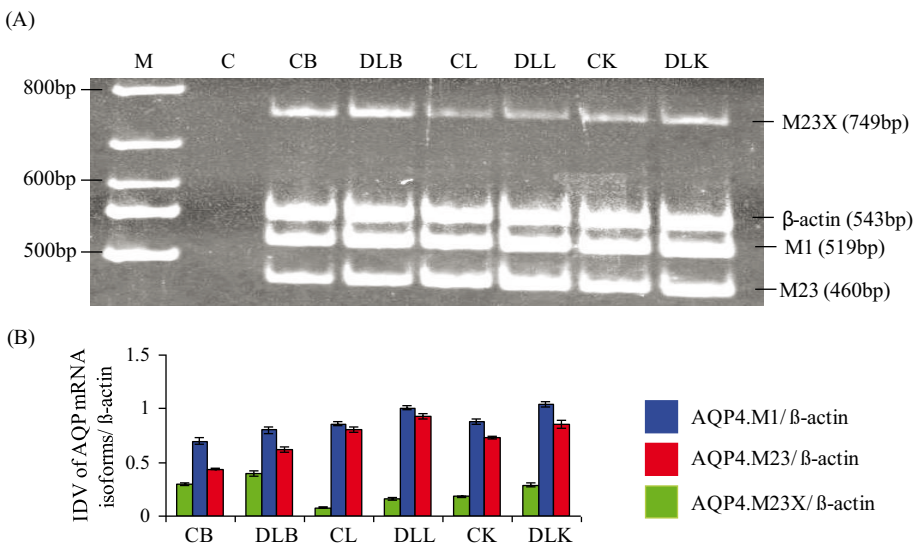

Figure 4. Semiquantization of AQP4 mRNAs expression in brain, lung, and kidney of DLA-challenged mice. (A) AQP4.M1, AQP4.M23, and AQP4.M23X expression in control brain (CB), control lung (CL), control kidney (CK) and Dalton's lymphoma brain (DLB), Dalton's lymphoma lung (DLL), Dalton's lymphoma kidney (DLK). (B) Histogram representing integrated density value of AQP4.M1, AQP4.M23, and AQP4.M23X, normalized against β-actin from three independent experiments ± SEM. M denotes marker 100-bp DNA ladder. C denotes negative control.

reaction for all three known transcripts of AQP4 in mice designed to study the impact of ascetic fluid introduction and development of Dalton's lymphoma and the impact on nonlymphatic tissues (brain, lung, and kidney) that abundantly express AQP4. The employment of MRT-PCR for the detection of transcripts and their quantification offers the advantages of high sensitivity and reproducibility. In addition, it helps with monitoring possible degradation of RNA and compensates for intra- and interassay variability during reverse transcription and PCR reactions. The use of an internal control for semiquantification of target transcripts offered the advantage of detection after RT-PCR, and it clearly indicates the success of RT and PCR steps. The amount of cDNA corresponding to the internal control was a good indicator of the degree of mRNA degradation and purity of the sample. The internal control compensates for the inherent interassay variability of RT-PCR. We used β-actin as an internal control because it is expressed at moderate levels in all types of body organs (An-hua et al., 2002).

Quantification of mRNA by MRT-PCR requires careful optimization at each step of the procedure, from RNA isolation up to coamplification of transcripts. Usually, 2 μg of RNA is enough for amplification of rare mRNA sequences. RNase should be properly taken care of, as it is a potential threat to isolated RNA. All solutions and buffers should be prepared in DEPC-treated water. Good quality and integrity of RNA is required for efficient amplification of PCR products. Furthermore, baking of glassware for 4 h at 250 °C and treatment of microtips, microfuge tubes, and gloves with DEPC are also useful. Conversation and the presence of crowds during the isolation of RNA and RT-PCR reactions should be completely avoided to prevent RNA degradation. The quality of RNA can be detected by the appearance of 28S (~5 kb) and 18S (~2 kb) RNA without smear by denaturing formaldehyde agarose gel electrophoresis. The band intensity of 28S RNA should be twice that of the 18S RNA band. The ratio of A260:A280 of extracted RNA should be 1.8 ± 0.1. Total RNA can be reverse transcribed into cDNA by random hexamers or oligo dT. We preferred random hexamers, because they prime from many matching sites on the RNA, increasing the chance of obtaining cDNA that encloses the target sequences. cDNA acts as a template to coamplify transcripts along with internal control using sequence-specific primers. Selection of efficient primers is essential for the success of MRT-PCR. Badly designed primers may result in poor or no amplification due to nonspecific products and primer–primer dimerization, which may become competitive enough to suppress one or more amplicon during coamplification. Therefore, choosing the right primers is the critical factor in developing a multiplex PCR system to overcome these problems. Primers must have unique sequences within the template DNA to be amplified. Simple rules can be followed for efficient primer selection. The two primer sequences should be selected from two different exons so that contaminating genomic DNA will give amplicons that are larger than amplicons from cDNA. Since both specificity and temperature and time of annealing are partly dependent on primer length, this parameter is critical for successful PCR (Kramer and Coen, 2001). Typically, primers 18–26 nucleotides in length are considered the best. GC content is an important feature of primers that provides information about the strength of annealing. All the forward and reverse primers used in coamplification should have similar GC content and melting temperature. In general, primers should have GC content between 40% and 60% to produce better results. Primers with 4 or more runs of Gs or Cs are generally avoided. Moreover, primer end complementarities and palindromes should not be incorporated so that they do not form hair pins. If this happens, a primer will fold back on itself, resulting in unproductive priming that decreases the overall signal obtained (Breslauer et al., 1986). Primers should not contain sequences that would allow one primer molecule to anneal itself or the other primers used in coamplification. The optimal melting temperature for primers should be 50–60 °C and should be comparable so that they all anneal at a similar time during coamplification. Even after efficient primer designing for coamplification, primer pairs should be checked separately at the optimal annealing temperature to produce their specific PCR products.

For quantification of gene expression, the number of PCR cycles should be optimized to fall into the exponential phases of the coamplification reactions for all amplicons. In our case, the exponential phases of AQP4.M1, AQP4.M23, AQP4.M23X, and β-actin amplifications are overlapping from cycles 24–34; we chose 29 cycles to amplify the targets in further multiplex reactions. We also measured the ratio between the intensity of each target fragment and the internal standard with an increasing amount of cDNA that did not change (data not shown), to ensure the same amount of cDNA template in coamplification reactions, because there is different cDNA synthesis efficiency in different experiments. To check the noninterference of multiple primers used to detect several different targets in a single PCR reaction, various combinations of primers should be used to check primer–primer compatibility. For AQP4 and β-actin transcripts, the primer–primer compatibility test revealed that the ratio was not affected by other primers or amplified products as a similar ratio between the normalized intensity of coamplified amplicons was obtained for every PCR reaction. A false positive signal may arise due to sparse contamination that could alter PCR sensitivity leading to potential problem;

it may sometimes pose a major limitation to users. In every PCR reaction, running a mock sample control and reverse transcriptase control is useful to exclude contamination artifacts. There must be a separate set of chemicals, reagents, and micropipettes for RT-PCR. We recommend a laboratory equipped with a separate setup of equipment and enzymes, chemicals, and buffers etc. To resolve the amplified products 6%–8% polyacrylamide can be used. Subsequently, ethidium bromide staining was performed. In this case ethidium bromide staining was efficient enough to detect the amplified products. However, radioisotope labeling of PCR products may be required in many cases to increase the detection efficiency of a low copy and rare transcripts. Additionally, in the case of poor or no amplification, RNA yield and quality and PCR conditions (annealing temperature, cycle numbers, primer–primer interaction) should be checked. If the problem persists, redesigning of primers is suggested. Moreover, in the case of nonspecific amplicon detection, the annealing temperature should be readjusted and primers redesigned if nonspecificity persists. Suppression of a few or all target amplicons by the most abundant amplicon in a multiplex reaction ensures that exponential phases for each primer pair are overlapping, if it is not possible to redesign the primers. If the problem persists, the PCR is run for a few cycles, optimized, and primers are added for the most abundant amplicon. We also acquired the suppressed band of all targets by internal control (β-actin). We added the primer pair of internal control after 10 cycles to obtain overlap of the exponential phases of all amplicons. Therefore, we suggest adding the primer pair of the most abundant amplicon after a few cycles of PCR. To check the reliability and reproducibility of our MRT-PCR assay, we studied the expression pattern of these AQP4 transcripts in mouse brain, lung, and kidney. AQP4 is a water-selective channel protein that is expressed in the brain, lung, kidney, etc. (Frigeri et al., 1995a, 1995b) and is involved in the regulation of water permeability in these organs (Chou et al., 1998; Manley et al., 2000; Song et al., 2000).

MRT-PCR is becoming increasingly popular because it is rapid, simple, sensitive, and relatively inexpensive. Other conventional methods for mRNA quantification such as northern blotting and ribonuclease protection assay lack sensitivity. Although real-time PCR is sensitive, it is still very expensive. The development of an efficient multiplex RT-PCR usually requires strategic planning and multiple attempts to optimize reaction conditions. Moreover, it is semiquantitative in nature and fails to determine the size of transcripts. Our findings suggest that MRT-PCR is a suitable alternative and has advantages over individual RT-PCR for the analysis of a single transcript in a single reaction.

Acknowledgments

RKG thanks the Council of Scientific and Industrial Research (CSIR), Government of India, for a Junior and Senior Research Fellowship (CSIR award no., file no.: 09/013 (0111) 2007– EMR I). Financial support to SP from the Center of Advanced Study in Zoology, UGC-UPE, University Grants Commission, DBT-ISLS Programs, Government of India, is gratefully acknowledged.

References

An-hua W, Walter LC (2002). Molecular cloning of the rat IL-13 alpha 2 receptor cDNA and its expression in rat tissues. J Neuro-Oncol 59: 99–105.

Bonab ZH, Farajnia S, Ghotaslou R, Nikkhah E (2012). Evaluation of nested PCR method for diagnosis of meningitis due to *Neisseria meningitidis* and *Haemophilus influenza*. Turk J Biol 36: 727–731.

Breslauer KJ, Frank R, Blöcker H, Marky LA (1986). Predicting DNA duplex stability from the base sequence. Proc Natl Acad Sci 83: 3746–3750.

Chou CL, Ma T, Yang B, Knepper MA, Verkman AS (1998). Fourfold reduction of water permeability in inner medullary collecting duct of aquaporin-4 knockout mice. Am J Physiol 274: C549–C554.

Crisan D (1994). Molecular diagnostic testing for determination of myeloid lineage in acute leukemia. Ann Clin Lab Sci 24: 355–363.

Frigeri A, Gropper MA, Turck CW, Verkman AS (1995a). Immunolocalization of the mercurial-insensitive water channel and glycerol intrinsic protein in epithelial cell plasma membranes. Proc Natl Acad Sci USA 92: 4328–4331.

Frigeri A, Gropper MA, Umenishi F, Kawashima M, Brown D, Verkman AS (1995b). Localization of MIWC and GLIP water channel homologs in neuromuscular, epithelial and glandular tissues. J Cell Sci 108: 2993–3002.

Gupta RK, Kanungo M (2013). Glial molecular alterations with mouse brain development and aging: up-regulation of the Kir4.1 and aquaporin-4. Age 35: 59–67.

Gupta RK, Prasad S (2013). Early down regulation of the glial Kir4.1 and GLT-1 expression in pericontusional cortex of the old male mice subjected to traumatic brain injury. Biogerontology 14: 531–541.

Gupta RK, Prasad S (2014). Differential regulation of GLT-1/EAAT2 gene expression by NF-κB and Nmyc in male mouse brain during postnatal development. Neurochem Res 39: 150–160.

Kleppe K, Ohtsuka E, Kleppe R, Molineux I, Khorana HG (1971). Studies on polynucleotides. XCVI. Repair replications of short synthetic DNA's as catalyzed by DNA polymerases. J Mol Biol 56: 341–361.

Kramer MF, Coen DM (2001). Enzymatic amplification of DNA by PCR: standard procedures and optimization. Curr Protoc Immonol doi: 10.1002/0471142735.im1020s24.

Kurnaz IA (2005). A gene expression study of the TGF-β signaling pathway components in differentiating PC12 cells. Turk J Biol 29: 189–195.

Li J, Qi S, Zhang C, Hu X, Shen H, Yang M, Wang J, Wang M, Xu W, Ma X (2013). A two-tube multiplex reverse transcription PCR assay for simultaneous detection of sixteen human respiratory virus types/subtypes. Biomed Res Int doi: 10.1155/2013/327620.

Ma T, Yang B, Verkman AS (1996). Gene structure, cDNA cloning, and expression of a mouse mercurial-insensitive water channel. Genomics 33: 382–388.

Manley GT, Fujimura M, Ma T, Noshita N, Filiz F, Bollen AW, Chan P, Verkman AS (2000). Aquaporin-4 deletion in mice reduces brain edema after acute water intoxication and ischemic stroke. Nat Med 6: 159–163.

Maurya AK, Vinayak M (2015). Quercetin regresses Dalton's lymphoma growth via suppression of PI3K/AKT signaling leading to upregulation of p53 and decrease in energy metabolism. Nutr Cancer doi: 10.1080/01635581.2015.990574.

Mullis KB (1990). Target amplification for DNA analysis by the polymerase chain reaction. Ann Biol Clin-Paris 48: 579–582.

Papadopoulos MC, Saadoun S (2015). Key roles of aquaporins in tumor biology. Biochim Biophys Acta doi: 10.1016/j.bbamem.2014.09.001.

Porob S, Nayak S, Fernandes A, Padmanabhan P, Patil BA, Meena RM, Ramaiah N (2013). PCR screening for the surfactin (sfp) gene in marine Bacillus strains and its molecular characterization from *Bacillus tequilensis* NIOS11. Turk J Biol 37: 212–221.

Song Y, Ma T, Matthay MA, Verkman AS (2000). Role of aquaporin-4 in airspace-to-capillary water permeability in intact mouse lung measured by a novel gravimetric method. J Gen Physiol 115: 17–27.

Surgun Y, Çöl B, Bürün B (2012). Genetic diversity and identification of some Turkish cotton genotypes (*Gossypium hirsutum* L.) by RAPD-PCR analysis. Turk J Biol 36: 143–150.

Tuo D, Shen W, Yang Y, Yan P, Li X, Zhou P (2014). Development and validation of a multiplex reverse transcription PCR assay for simultaneous detection of three papaya viruses. Viruses 6: 3893–3906.

Verma P, Singh P, Gandhi BS (2013). Prophylactic efficacy of *Bacopa monnieri* on decabromodiphenyl ether (PBDE-209)-induced alterations in oxidative status and spatial memory in mice. Asian J Pharm Clin Res 6: 242–247.